CUMENTATION PAGE

Form Approved
OMB No 0704-0188

AD-A232 205

1b RESTRICTIVE MARKINGS

	3. DISTRIBUTION / AVAILABILITY OF REPORT
2b. DECLASSIFICATION / DOWNGRADING SCHEDULE	Approved for public release; Distribution unlimited

4 PERFORMING ORGANIZATION REPORT NUMBER(S)	5 MONITORING ORGANIZATION REPORT NUMBER(S)
PL-TR-91-2021	

6a. NAME OF PERFORMING ORGANIZATION	6b OFFICE SYMBOL (If applicable)	7a NAME OF MONITORING ORGANIZATION
Phillips Laboratory Geophysics Directorate	PHG	

6c ADDRESS (City, State, and ZIP Code)	7b ADDRESS (City, State, and ZIP Code)
Hanscom AFB Massachusetts 01731-5000	

8a NAME OF FUNDING / SPONSORING ORGANIZATION	8b OFFICE SYMBOL (If applicable)	9 PROCUREMENT INSTRUMENT IDENTIFICATION NUMBER

8c. ADDRESS (City, State, and ZIP Code)	10 SOURCE OF FUNDING NUMBERS			
	PROGRAM ELEMENT NO	PROJECT NO	TASK NO	WORK UNIT ACCESSION NO
	61102F	2311	G5	01

11. TITLE (Include Security Classification)
A Test of Convection Models for IMF B_z North

12. PERSONAL AUTHOR(S)
N.C. Maynard, J.J. Sojka*, R.W. Schunk*, J.P. Heppner**, L.H. Brace**

13a. TYPE OF REPORT	13b TIME COVERED	14 DATE OF REPORT (Year, Month, Day)	15 PAGE COUNT
Reprint	FROM _____ TO _____	1991 January 30	13

16 SUPPLEMENTARY NOTATION *Utah State University, Logan, Utah 84322 **Goddard Space Flight Center, Greenbelt, MD 20771 – Reprinted from Planet Space Sci., Vol. 38, No. 9 pp. 1077-1089, 1990

17.	COSATI CODES		18. SUBJECT TERMS (Continue on reverse if necessary and identify by block number)
FIELD	GROUP	SUB-GROUP	Electro magnetosphere, Convection models, Electron precipitation

19. ABSTRACT (Continue on reverse if necessary and identify by block number)

Abstract—Plasma convection at high latitudes is strongly controlled by the direction of the interplanetary magnetic field (IMF). When the IMF is southward, two-cell convection patterns exist with anti-sunward flow in the polar cap and return flow equatorward in the auroral oval. When the IMF is northward, however, the situation is more complicated and several convection patterns have been proposed to explain the observations of sunward polar cap flow, including three-cell, four-cell, and distorted two-cell patterns. Since the different convection patterns are expected to display different ionospheric signatures, the Utah State University Ionospheric Model can provide insight as to which convection model applies to given situations. The model was run to obtain diurnally reproducible ionospheric densities and temperatures for summer and winter conditions using both distorted two-cell and three-cell convection patterns. Differences due to the different convection patterns manifest themselves in the depth and location of polar holes in the F-region electron density. While the total depth of the model holes is a characteristic of the diurnally reproducible pattern, the features appear and are recognizable within 0.5 h. Langmuir probe data from 41 DE-2 passes, during which the IMF B_z component was northward, have been qualitatively checked against the model predictions. The cross polar cap electron density profiles of a large majority of the passes more closely conform to the distorted two-cell runs for both polarities of the IMF B_y component. This test can be generalized to rule out proposed convection patterns based on the presence/absence and position of polar electron density holes.

20 DISTRIBUTION / AVAILABILITY OF ABSTRACT	21 ABSTRACT SECURITY CLASSIFICATION
☐ UNCLASSIFIED/UNLIMITED ☒ SAME AS RPT ☐ DTIC USERS	Unclassified
22a NAME OF RESPONSIBLE INDIVIDUAL	22b TELEPHONE (Include Area Code)	22c OFFICE SYMBOL
N.C. Maynard	(617) 377-2431	PHG

DD Form 1473, JUN 86   Previous editions are obsolete.   SECURITY CLASSIFICATION OF THIS PAGE

Unclassified

A TEST OF CONVECTION MODELS FOR
IMF B_z NORTH

N. C. MAYNARD
Geophysics Laboratory, Hanscom AFB, MA 01731, U.S.A.

J. J. SOJKA and R. W. SCHUNK
Utah State University, Logan, Utah 84322, U.S.A.

and

J. P. HEPPNER* and L. H. BRACE
Goddard Space Flight Center, Greenbelt, MD 20771, U.S.A.

Abstract—Plasma convection at high latitudes is strongly controlled by the direction of the interplanetary magnetic field (IMF). When the IMF is southward, two-cell convection patterns exist with anti-sunward flow in the polar cap and return flow equatorward in the auroral oval. When the IMF is northward, however, the situation is more complicated and several convection patterns have been proposed to explain the observations of sunward polar cap flow, including three-cell, four-cell, and distorted two-cell patterns. Since the different convection patterns are expected to display different ionospheric signatures, the Utah State University Ionospheric Model can provide insight as to which convection model applies to given situations. The model was run to obtain diurnally reproducible ionospheric densities and temperatures for summer and winter conditions using both distorted two-cell and three-cell convection patterns. Differences due to the different convection patterns manifest themselves in the depth and location of polar holes in the F-region electron density. While the total depth of the model holes is a characteristic of the diurnally reproducible pattern, the features appear and are recognizable within 0.5 h. Langmuir probe data from 41 *DE*-2 passes, during which the IMF B_z component was northward, have been qualitatively checked against the model predictions. The cross polar cap electron density profiles of a large majority of the passes more closely conform to the distorted two-cell runs for both polarities of the IMF B_y component. This test can be generalized to rule out proposed convection patterns based on the presence/absence and position of polar electron density holes.

INTRODUCTION

Under northward interplanetary magnetic field (IMF) conditions electric fields in the polar cap (i.e. the region poleward of the auroral belt, that is commonly characterized under southward IMF conditions by dawn–dusk electric fields and anti-sunward convection) are often highly structured with a variety of irregularity dimensions. The irregularities often include structures in which the sign of the dawn–dusk electric field component is reversed, producing sunward convective motion. Large-scale, distinct regions in which the fields are predominantly of one sign, and which may be identified with convection cells may or may not be present.

Previous models of convective electric fields for northward IMF have proposed patterns with variable numbers of cells. Crooker (1979), in studies of allowed merging regions, postulated a large convection cell

associated with the polar cap and the lobes of the magnetosphere for IMF B_z North conditions. Circulation in the cell changed direction with IMF B_y. For strong northward IMF, the cell was concentrated on one side or the other of the polar cap depending on the size of B_y. The concept of a four-cell pattern was introduced by Burke *et al.* (1979) to explain the *S3*-2 satellite observation of sunward convection in the center of the polar cap. Reiff and Burch (1985) proposed a four-cell pattern with two lobe cells in the polar cap and two narrow cells at adjacent lower latitudes driven by viscous interaction in the boundary layer. One lobe cell could dominate the other depending on the strength and polarity of the B_y component. For strongly positive B_z, one of the lobe cells in each cap was driven while the other was a reclosure cell on closed field lines driven by merging in the opposite polar cap. Heelis *et al.* (1986) also postulated four-cell patterns with the dominant lobe cell being dependent on the B_y component. Banks *et al.* (1984) and Clauer and Banks (1986) developed convection patterns having four cells that were related to the

---

* Present address: BDM International Inc., 9705 Patuxent Woods Drive, Columbia, MD 21406, U.S.A.

dayside cusp region based on direct coupling of solar wind electric fields into DPY and DPZ related current systems. Their model resulted in two extra small cells appearing in the vicinity of the cusp, but not extending back into the polar cap. Sojka *et al.* (1986) developed a mathematical model with a K_p dependence that can be adjusted to produce two, three or four cells depending on the IMF conditions. The above models concentrated on explaining phenomena on the dayside of the polar cap, and these patterns were loosely closed or left open on the nightside. Kan and Burke (1985) tried to address the nightside closure while still keeping the four-cell pattern by invoking instabilities and wave-like structures in the nightside. However, none of the above three- and four-cell patterns easily address the persistence of the Harang discontinuity during both quiet and B_z North conditions (Maynard, 1974; Heppner and Maynard, 1987).

Heppner and Maynard (1987) empirically derived typical patterns for northward IMF conditions for selected passes from the *DE*-2 electric field data set (Maynard *et al.*, 1981) in which the IMF, as determined from *ISEE* 3, was clearly unambiguous. These patterns represented distortions of the two-cell patterns derived for southward IMF conditions (Heppner and Maynard, 1987). The distortions were such that the evening convection cell rotated into or around the morning cell. The distortion increased with an increase in the magnitude of the northward IMF component. In addressing the question of how the convection patterns close on the nightside, the distorted two-cell pattern was the only one that consistently matched the data for the large majority of cases.

This poses a dilemma in deciding which convection pattern is appropriate when based on any one orbit of data. For instance, Killeen *et al.* (1985), following the Burke *et al.* (1979) and Potemra *et al.* (1984) interpretation of a "W" pattern as indicative of four cells, explained a series of passes during strong B_z North conditions in terms of four-cell patterns. Heppner and Maynard (1987) showed that those same passes also fit the distorted two-cell models. It would be desirable to be able to have additional tests to aid in the selection of the best interpretation.

The Utah State Ionospheric Model (see Schunk, 1988) provides a global description of the ionosphere based on input parameters, one of which is a global ion convection pattern. The model plasma densities are sensitive to the past convective history of a flux tube. A flux tube which does not encounter a source of ionization such as the sunlit dayside or the auroral region will quickly become depleted. Thus, convection patterns which have central portions of cells which only circulate within the polar cap will cause electron

density holes to develop in the polar cap. Evidence of these holes will start to develop within 0.5 h of a pattern change. Sojka and Schunk (1987), in a study of the response of the ionosphere to B_z North convection patterns, caused two electron density holes to develop by driving the ionospheric model with a theoretical four-cell pattern. By applying this approach using different convection patterns as a driver, one can obtain predictions of the electron density patterns in the high latitude ionosphere. These density predictions can then be qualitatively compared with measurements of electron density such as those from the *DE*-2 Langmuir probe. In this way a "blind" test of the applicability of a particular convection pattern can be performed with the density data being used as the discriminator.

The purpose of this paper is (1) to test whether distorted two-cell patterns or multicell patterns are most applicable under relatively stable B_z North input conditions using the Utah State ionospheric model and *DE*-2 Langmuir probe data, and (2) to demonstrate that such a blind test can be used to restrict the options for convection pattern configurations for a given situation. For this test the Utah State ionospheric model was driven with the Heppner–Maynard (1987) distorted two-cell model and with the Sojka *et al.* (1986) three-cell model as an example of multicells. No other input conditions were varied. The Sojka *et al.* model was chosen to keep the similarity in the patterns as close as possible as explained below. Times were chosen for comparison with the simulations in which the IMF was stably configured and when *DE*-2 data were available. Forty-one cases were considered. The results of this test, which favor the distorted two-cell model, will be generalized in the Discussion to conclude that for individual satellite passes the presence/absence and position of polar electron density holes can be used to discriminate against, or rule out, specific convection patterns. As an example, the test is applied to the patterns presented in the theta aurora paper of Frank *et al.* (1986).

IONOSPHERIC MODEL

The ionospheric model adopted for this study was originally developed as a mid-latitude multi-ion (NO^+, O_2^+, N_2^+, O^+) model by Schunk and Walker (1973), and was later extended to include high latitude effects due to convection electric fields and particle precipitation by Schunk *et al.* (1975). A further extension of the model to include the minor ions N^+ and He^+, an updated photochemical scheme, and the MSIS atmospheric model (Hedin *et al.*, 1977) is

described in Schunk and Raitt (1980). More recently, the ionospheric model has been extended by Schunk and Sojka (1982) and Schunk et al. (1986) to include thermal conduction and diffusion-thermal heat flow, so that the ion and electron temperatures are now rigorously calculated at all altitudes between 120 and 800 km.

In the high latitude model, flux tubes of plasma are followed as they convect through a moving neutral atmosphere. For each flux tube, altitude profiles of the ion and electron temperatures and the NO^+, O_2^+, N_2^+, N^+, O^+, and He^+ densities are obtained by solving the appropriate continuity, momentum, and energy equations including all of the high latitude processes thought to be important. The equations are solved over the altitude range from 120 to 800 km, with boundary conditions specified at the lower and upper ends of the flux tubes. For densities, chemical equilibrium is assumed at 120 km and no escape flux is assumed at 800 km. For temperatures, local thermal coupling is assumed at 120 km and a specified heat flux is assumed at 800 km. For this study, the electron and ion heat fluxes through the upper boundary were taken to be zero.

Three-dimensional density and temperature distributions are obtained by following many flux tubes of plasma and by keeping track of their locations as a function of time. In this study, all runs exceeded 24 h in duration to ensure that equilibrium was reached for the normal diurnal variation for each of the cases considered.

The ionospheric model does not self-consistently couple to the magnetosphere and thermosphere and, hence, a number of inputs are required for a given run. The model requires global distributions for the neutral densities, temperature, and wind. At high latitudes, the model also requires the magnetospheric (convection) electric field pattern and a description of the auroral electron energy flux. These important thermospheric and magnetospheric inputs vary from one study to another; those adopted for this study are described in the following two sections of the paper. A complete description of the USU Ionospheric Model is given by Schunk (1988) and the reader is referred to this article for further details. A comprehensive review of the model-data comparisons and model applications that have been conducted to date is given by Sojka (1989).

IONOSPHERIC INPUTS

Since this study is designed to contrast two types of convection models and their effects on the ionosphere,

the other input parameters in the model were set for specific solar cycle, seasonal and magnetic conditions and held constant for the runs with each convection pattern. Table 1 lists these parameters. For the neutral atmosphere the MSIS model (Hedin et al., 1977) was used, while for the neutral winds a simple pattern with anti-sunward flow across the polar cap with a speed of about 200 m s^{-1} was adopted. This pattern has been used in several previous studies with the ionospheric model and is described in Sojka et al. (1981).

Electron precipitation in the auroral oval acts as a plasma production source, a source of bulk electron heat, and a source of energy that flows through the model's upper boundary. The empirical precipitation model developed by Hardy et al. (1985) has been used. The magnetic activity (K_p) used as an input in the Hardy et al. model is given in Table 1. The convection and precipitation patterns were chosen such that they overlapped as closely as possible. The procedure for calculating the ionization rate and the thermal electron bulk heating rate from the auroral electron energy flux is described by Schunk (1988).

CONVECTION MODELS

In order to make the test as "blind" as possible, the convection models selected were not keyed to actual data, but were based on the IMF conditions at the time of a DE-2 pass. In the high-latitude ionosphere, the convective history of a flux tube is a major influence for determining its electron density. Thus, the total convection pattern, not the detail along the satellite pass, becomes the controlling factor. Figure 1, for IMF northward and B_y positive, shows the electric potentials associated with the Northern Hemisphere distorted two-cell model of Heppner and Maynard (1987), left panel, and that of the three-cell model of Sojka et al. (1986), right panel, which is chosen as a representative of multiple cell models. The potential is represented by contours drawn at 2 kV intervals in a magnetic latitude-M.L.T. coordinate system. Negative potentials are shown as dashed curves. Figure 2 shows the corresponding Northern Hemisphere patterns for IMF northward and B_y negative. The models were adjusted so as to make their auroral regions coincide. The three-cell model was chosen to provide a path of strong anti-sunward convection on the appropriate side of the polar cap in order to conform most closely with its accompanying distorted two-cell model. The rest of the polar cap was allowed to vary according to the model.

Differences between the two convection models are evident, especially in the noon and midnight sectors; however, certain similarities exist. Strong anti-sun-

TABLE 1. USU IONOSPHERIC MODEL INPUTS

Input parameter	Winter	Summer
Year month/day	22 Dec. 1982	22 June 1982
Solar F10.7	210	210
Magnetic activity K_p	1	1
Magnetic activity A_p	8	8
Auroral precipitation	Hardy oval ($K_p = 1$)	Hardy oval ($K_p = 1$)
Electric field distorted 2 cells	Heppner and Maynard	Heppner and Maynard
Electric field multicells	Sojka *et al.*	Sojka *et al.*
Northward IMF B_z	15	15
B_y	±15	±15

ward convection occurs at the dusk side of the polar cap for B_y negative and at the dawn side for B_y positive and the auroral zones are similar. Note that while the Sojka *et al.* (1986) model has a convection cell that circulates only entirely within the polar cap, the distorted two-cell equipotentials return to the auroral oval for each circulation. This also results in a stronger sunward flow within the polar cap in the three-cell models than in the distorted two-cell models. The selection of the Sojka *et al.* three-cell model as the representative of multicell models was done to maximize the similarities between the distorted two-cell models and the multicell models. More cells within the polar cap would have increased the differences between the multicell and the Heppner–Maynard distorted two-cell models and, as shown by Sojka and Schunk (1987), would have increased the number of polar holes created by the model in the electron density patterns.

RESULTS AND COMPARISONS

A total of 41 satellite crossings of the polar region which had stable IMF conditions, were selected for study. The DE-2 passes were selected from those used by Heppner and Maynard (1987) in the derivation of the distorted two-cell models and represent cases in which the IMF direction as determined from *ISEE* 3 data was stably configured from 1 5 h before the pass to 30 min before the pass to ensure that the IMF conditions were unambiguous. These passes represented a readily accessible data set. Any individual pass can be represented by many solutions for the global potential pattern. Because the test did not fine tune the models to individual passes and because the Heppner–Maynard models are meant to be average patterns and not represent any one pass exactly, the use of these passes does not introduce a significant bias in the results. The initial scan used appropriate winter, summer or equinox conditions in which the

ionospheric model was run to equilibrium. The appropriate universal time was then selected for the model-to-data comparisons. For a selected group of orbits the model was rerun to match more closely the sunspot number and convection pattern size. Examples presented in the paper are from that subset.

Before presenting model-data comparisons, it is important to note that the ionospheric model was run to obtain diurnally reproducible density features. In this case, the ionosphere has sufficient time to fully adjust to the driving convection pattern and, hence, the distinguishing density features associated with the convection pattern will be well developed. In practice, however, B_z will not remain steady for a 24-h period. Nevertheless, when the IMF changes direction, the time constant for corresponding density changes is of the order of 0.5 h. It is within this time period that the distinguishing density features should start to appear, although they may not be as well developed as the equilibrium solutions predict. For this reason, and also considering that the convection patterns are not exact in the representation of actual conditions, only a qualitative comparison between model predictions and measurements is possible.

Figure 3 presents a comparison of results from a winter case in which B_y was positive. The model densities for the different convection patterns are presented on the left. The top polar dial, encompassing from 50 magnetic latitude to the pole, displays oxygen ion densities at 800 km (approximately equivalent to total density) for the Heppner Maynard pattern run, while the bottom polar dial shows the oxygen ion density for the multicell pattern run. The DE-2 track is given by the dark line across the plot from dawn to dusk. The measured electron density, N_e, and temperature. T_e (Krehbiel *et al.* 1981), and horizontal electric field along the orbit track, E_y (Maynard *et al.* 1981), from DE-2 is shown on the right. The altitude for this pass is near 700 km in the center of the polar cap. The comparisons were done qualitatively

IMF Bz NORTH B_y POSITIVE
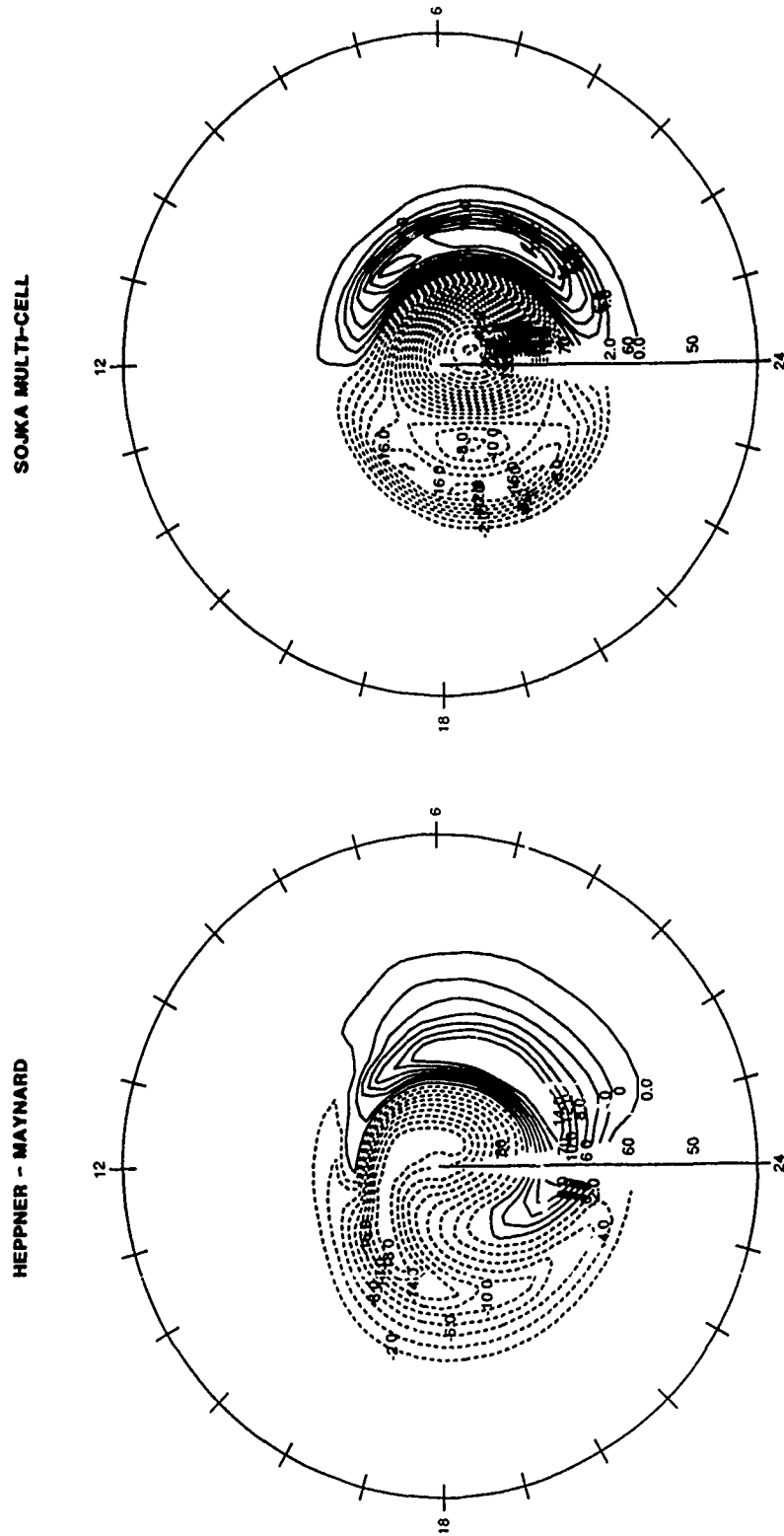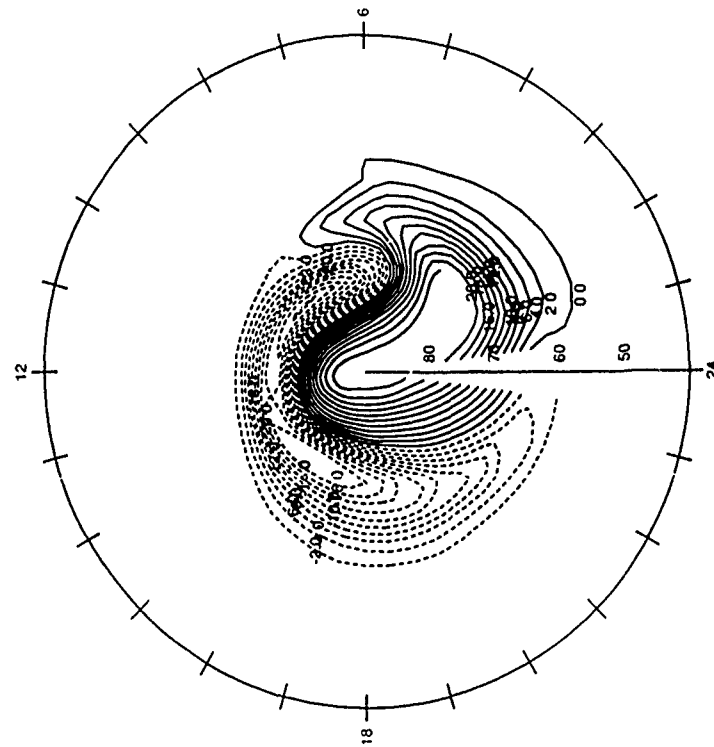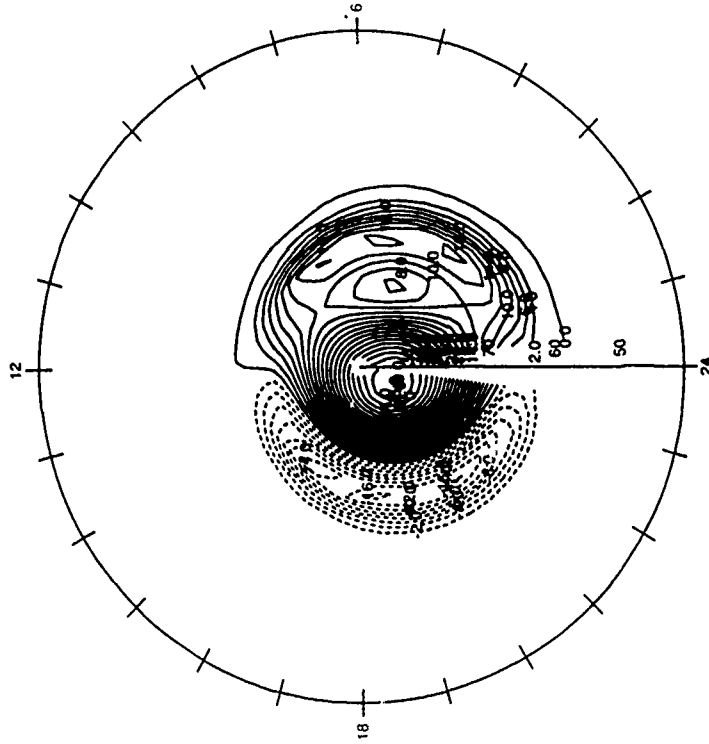
HEPPNER – MAYNARD

SOJKA MULTI-CELL

FIG. 1. ELECTRIC POTENTIAL CONTOURS FOR THE NORTHERN HEMISPHERE ASSOCIATED WITH THE HEPPNER AND MAYNARD (1987), LEFT PANEL, AND THE SOJKA *et al.* (1986), RIGHT PANEL, MODELS FOR IMF NORTHWARD AND B_y POSITIVE CONDITIONS. The potentials are contoured at 2 kV intervals in a magnetic latitude–M.L.T. coordinate system.

IMF Bz NORTH B_y NEGATIVE

HEPPNER – MAYNARD

SOJKA MULTI-CELL

FIG. 2. ELECTRIC POTENTIAL CONTOURS FOR THE NORTHERN HEMISPHERE ASSOCIATED WITH THE HEPPNER AND MAYNARD (1987), LEFT PANEL, AND THE SOJKA *et al.* (1986), RIGHT PANEL, MODELS FOR IMF NORTHWARD AND B_y NEGATIVE CONDITIONS.
The potentials are contoured at 2 kV intervals in a magnetic latitude M.L.T. coordinate system.
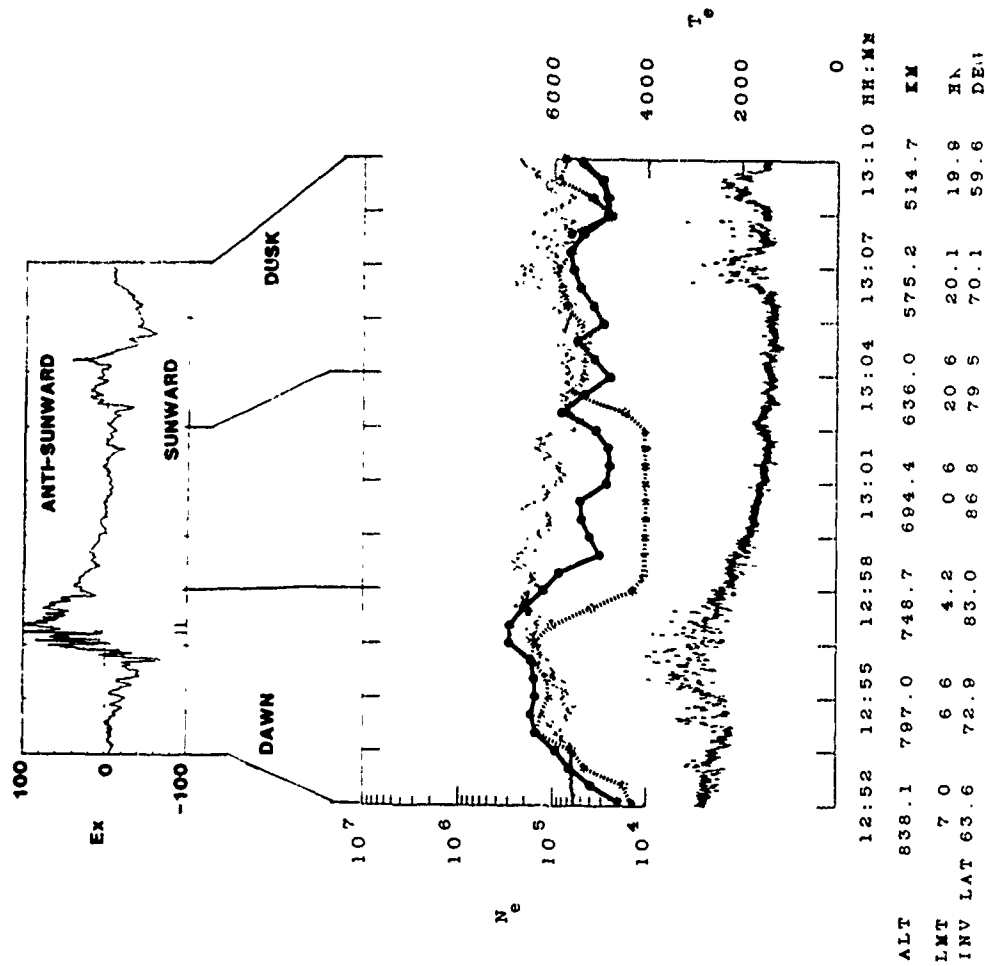
DE-2 ORBIT 1554 81320

IMF B_y (positive) winter

Heppner Maynard

Multicell

FIG. 3 (COMPARISON OF MODELLED AND OBSERVED PLASMA DENSITY FOR IMF NORTHWARD AND B POSITIVE CONDITIONS. Model I results are shown as color coded polar dial plots, at the left of the figure. The top dial corresponds to a X at 800 km for the Heppner and Maynard (1987) convection model run, while the bottom dial corresponds to the Sojka et al. (1986) convection model run. The satellite trajectory is shown in the dial plots. The observed I, electric field component, X, and I, along this DE-2 trajectory are shown in line plots to the right. The heavy solid and dotted lines on the density plot show densities along the trajectory of DE-2 calculated, respectively, from using the Heppner Maynard and distorted two cell model and the multicell model to drive the ionospheric model)
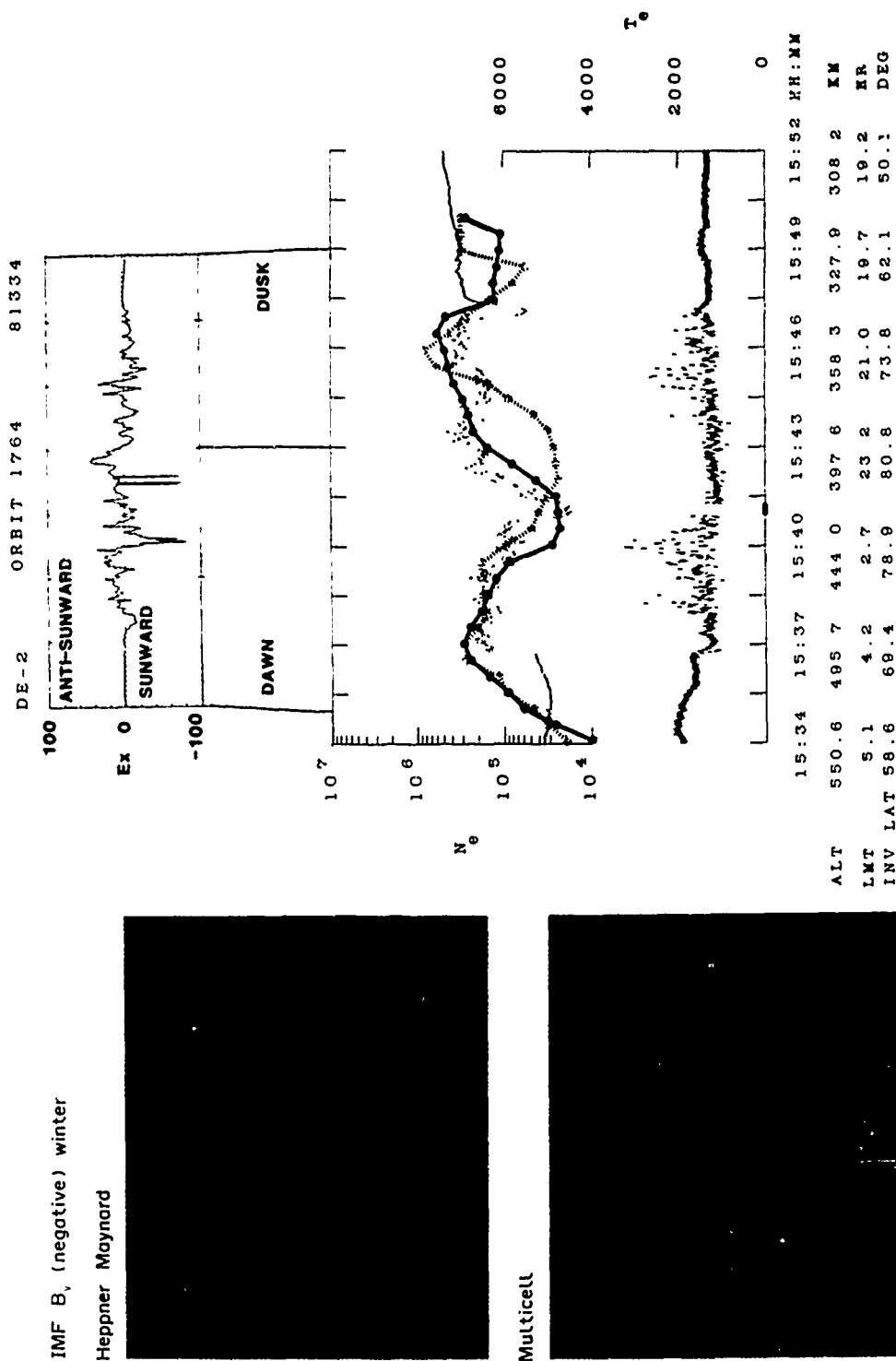
FIG. 4 COMPARISON OF MODELED AND OBSERVED WINTER ELECTRON DENSITIES FOR IMF NORTHWARD AND B NEGATIVE CONDITIONS. The Format of this figure is identical to Fig. 3 except that the model-produced densities in the polar plots are for 300 km, to more closely correspond to the data

between the global patterns and the density traces. However, in order to show clearly the differences and similarities, the heavy solid and dotted lines in the density plot are actual values along the orbit track calculated from the ionospheric model runs using the Heppner–Maynard distorted two-cell and multicell models, respectively. The model results using the multicell pattern show a deep hole in the center of the polar cap. Both model runs have an enhanced morning side; however the Heppner–Maynard distorted two-cell run does not have a deep hole in the polar cap, showing only a small reduction at the edge of the auroral zone. Correspondingly, the measured electron density is highest on the morning side of the polar cap, with the high density region extending to the noon–midnight meridian. This is the region of the highest anti-sunward convection speeds both in the data and in the models, bringing highly populated flux tubes from the sunlit dayside region to the polar cap. The lack of a significant hole in the measured density at the pole is obvious. In this respect the measured density profile best fits the density results obtained using the Heppner–Maynard convection model.

Figure 4 shows an example in the same format for B_z negative. In this case the satellite altitude at the center of the polar cap is near 400 km. The polar dials depict the electron density at 300 km from the model runs. Note that both convection patterns produce polar holes. For the distorted two-cell pattern, the hole is centered on the morning side of the noon–midnight meridian, while for the multicell pattern the hole is centered slightly to the evening side of the noon–midnight meridian. The measured electron density profile in Fig. 4 shows a deep hole on the morning side of the noon–midnight meridian plus a smaller hole on the equatorward edge of the evening auroral region (seen in both models). This lower latitude hole is the midlatitude trough (Spiro et al., 1978). The electric field in this case is more irregular, but still has an overall pattern consistent with the distorted two-cell pattern. The density data fit the distorted two-cell driven results better, as can be seen by comparison with the heavy lines which show the model results along the orbit track.

The two examples favor the Heppner–Maynard distorted two-cell patterns very strongly. Each of the 41 passes was compared with the model results, and the agreement was categorized as being strongly in favor of, moderately in favor of, or weakly in favor of the appropriate convection driver. Two other categories were required. First, several passes were fitted equally well by both models and were categorized as "no choice". In several of the passes for B_z negative, neither convection pattern provided reasonable com-

parisons and these passes were judged as "other". Some of the passes categorized as "other" were passes where the size of the auroral oval and polar cap was much larger than that used in the models due to an extremely large total magnitude of the IMF. In addition, lack of full agreement in many cases could be expected, since only the most distorted convection patterns were used in the ionosphere model runs even though the less distorted patterns might in some cases have been more applicable. The results are presented in a bar graph in Fig. 5. A full spectrum of cases is seen; however, a majority of the cases (23) favor to some degree the Heppner–Maynard distorted two-cell model. Ten of the 41 passes considered strongly favored the distorted two-cell patterns. When the no decision cases are omitted, the results are even more strikingly in favor of the distorted two-cell model (23 of 29).

DISCUSSION

To put the above results in perspective, this test only compared the Heppner–Maynard distorted two-cell model against the Sojka et al. three-cell model. The passes studied were from the group which had stable IMF conditions and had been used to derive the distorted two-cell patterns (as explained earlier, this was not considered a biasing factor). While the results were clearly in favor of the distorted two-cell model used, they do not a posteriori favor all distorted two-cell models over all multicell models. However, certain characteristics of the comparisons do lend themselves to generalization.

The primary distinguishing characteristics used to categorize the agreement, or lack thereof, were the depth and position of polar cap holes in the electron density. The polar cap holes are produced in the ionospheric model when magnetic flux tubes circulate only within the polar cap (i.e. on equipotential contours that are confined to the polar cap), and particularly when these flux tubes remain in darkness. In the $-B_z$ case the distorted two-cell pattern develops a hole because of the weak ionization levels encountered when the circulating flux tubes contact the post-midnight auroral oval. The holes are deepest at universal times when the terminator is farthest toward the dayside of the magnetic pole. The choice between the convection patterns depends on the location of the hole and is, therefore, model sensitive. For instance, the Sojka and Schunk (1987) four-cell pattern created two holes in the center of the polar cap because two of the cells had centers that only circulated in the polar cap. Different distorted two-cell or multicell patterns could result in changes in the location, size and or
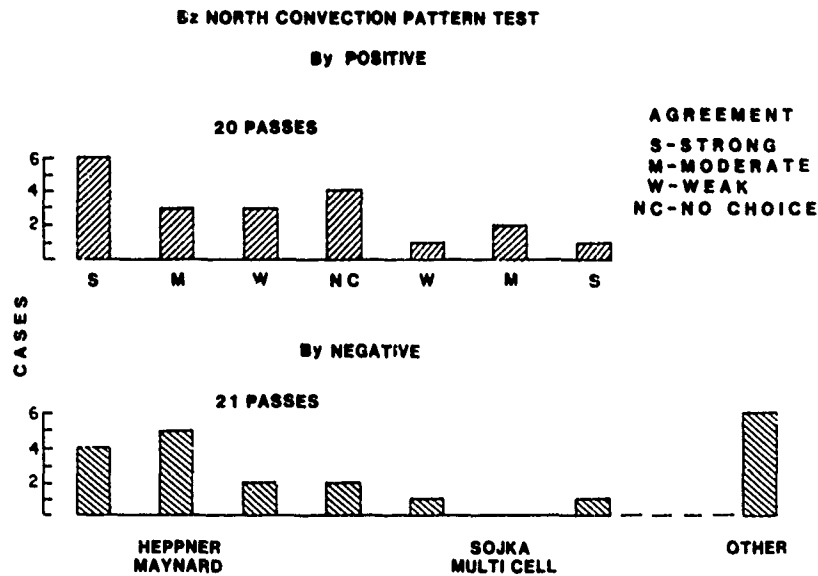
Bz NORTH CONVECTION PATTERN TEST

By POSITIVE

FIG 5. STATISTICAL COMPARISON OF DE-2 ELECTRON DENSITY DATA WITH MODEL RESULTS FOR A NORTHWARD IMF WITH B_z POSITIVE (TOP PANEL) AND B_z NEGATIVE (BOTTOM PANEL).
The seven histograms associated with each panel represent, from left to right, the following conditions: strongly in favor of, moderately in favor of, weakly in favor of the Heppner–Maynard (1987) model, equally likely; and then weakly in favor of, moderately in favor of, and strongly in favor of the Sojka et al. (1986) model. Of a total of 41 data sets, six could not be grouped according to these descriptions and, hence, are in the "other" group.

existence of holes and, therefore, changes in the comparison statistics.

Thus, the presence or absence and the position of holes in the electron density in the polar cap can be used as a criterion to rule out possible convection patterns. For example, in Fig. 3 for Northern Hemisphere B_z·, the distorted two-cell pattern does not produce a clear hole, whereas the multicell pattern does. No hole is observed. Any other convection models that have large cells whose centers only circulate within the polar cap will not fit the observed data. Also the dawn side electron densities in the polar cap require significant anti-sunward flow from the highly ionized dayside in this B_z· case. Both of these features are more easily satisfied by the distorted two-cell patterns.

The case that most favored the multicell pattern in the B_z data set (not shown) involved a condition in which B_z was nearly zero and the principal horizontal component was in B_y. The distorted two-cell pattern breaks down in this situation of $B_z \gg |B_z|$, either from the distortions during transition between the patterns or from a different forcing function. This IMF condition produced a four-cell pattern in the study of Clauer and Friis-Christensen (1988).

Some cases were found where neither pattern could

be adapted. These were generally cases where the patterns were not sized correctly due to an abnormally high B_z, or cases where the potential data were extremely variable and bore no resemblance to the model patterns. Thus, no one set of patterns will represent all conditions. However, the distorted two-cell concept offers a new approach to changing from B_z South to B_z North conditions in a smooth manner. It does not cover the case when the electric field is so variable that no background convection pattern can be discerned. Hoffman et al. (1988) found for quiet conditions with B_z North that a pattern was recognizable in the electric field 60% of the time, even in their generally weakly-driven cases. Also, it should be noted that during northward IMF conditions some precipitation is present in the polar cap. However, for the ionospheric model runs, polar cap precipitation was not included because it was not clear how to incorporate it in the Hardy et al. (1985) precipitation model.

The above generalization restricting the topology of convection patterns based on the existence and position of holes in the electron density in the polar cap can be applied to the theta aurora passes presented by Frank et al. (1986) to test the multicell patterns which were interpreted from the ion drift data. Three
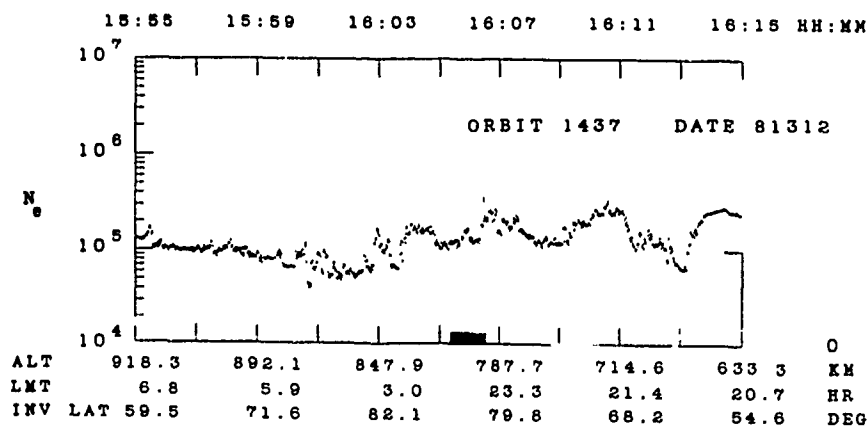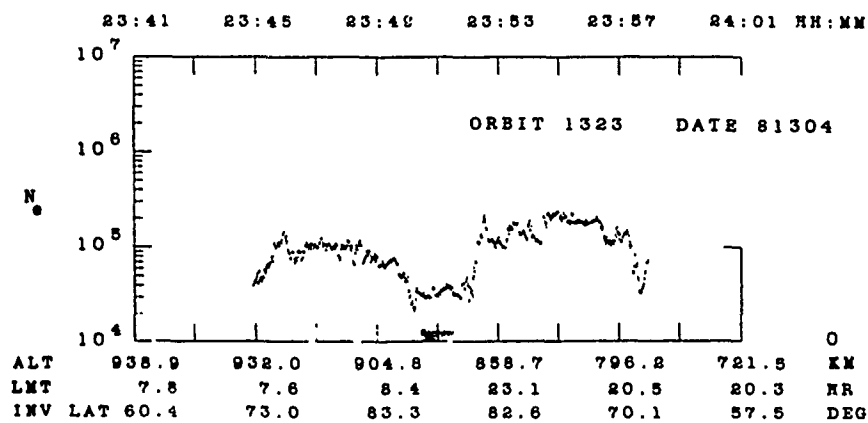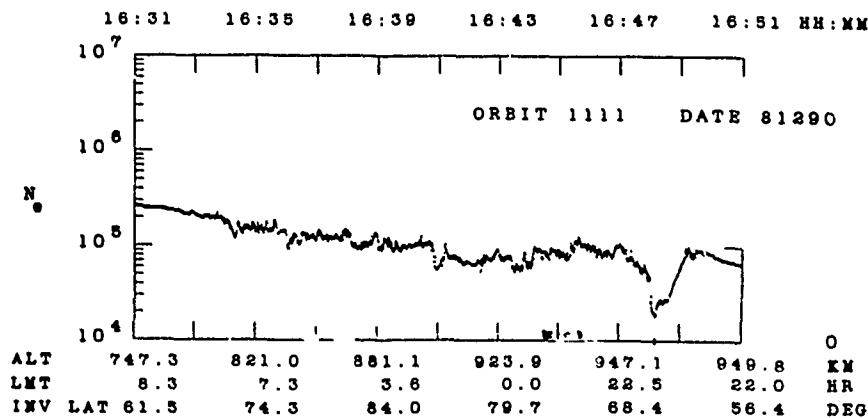
FIG. 5. *DE*-2 ELECTRON DENSITY PLOTS FOR THREE OF THE THETA AURORA PASSES DISCUSSED BY FRANK *et al*
(1986)
The black bar on the horizontal axis of each plot denotes the location of the auroral emission identified
as the theta bar.

passes were identified as having multicell patterns. Passes 1437 (8 November 1981) and 1323 (31 October 1981) were for B_y negative conditions. Note that for pass 1437 B_y was only weakly positive. For pass 1111 (17 October 1981) the B_y component was variable. Figure 6 shows the $L\bar{z}$-2 electron density plots for these passes. Only orbit 1323 shows a clear polar hole. The hole is somewhat to the morning side of the noon–midnight line. In comparing with Fig. 4 and the discussion of that figure, this would favor the distorted two-cell pattern over the three-cell pattern. Frank *et al.* (1986: Figs 11 and 7) show a polar cell on the evening side and an indeterminate structure on the morning side. Since their evening cell could not produce the observed hole, this test rules out their pattern. Pass 1111 has almost no discernable density structure. It tracks from about 9 to 21 h, passing through holes for either B_y condition for the multicell runs in Figs 3 and 4. The orbit track would just touch the top of the hole for B_y negative, and there is no hole for B_y positive in the distorted two-cell runs. The lack of a deep hole could be attributed to the near equinox conditions which would result in more of the cap being in sunlight. However, even in summer, the multicell convection driven model run showed some depletion. The lack of density structure is inconsistent with the multicell pattern proposed by Frank *et al.* (1986: Figs 12 and 9). For pass 1437 no large polar hole is seen; however, dips of the order of a factor of two or less are seen in the evening side of the polar cap and in the vicinity of the theta bar. The Sojka and Schunk (1987) four-cell hypothetical model for a theta aurora condition had a ridge (not a dip) separating the two polar holes partly due to particle production from electron precipitation at a simulated theta aurora location. This pass does not agree well with either of the simulations in this test, although there is certainly no evidence of having crossed cells with circulation only within the polar cap, as could be inferred from the pattern for this pass given by Frank *et al.* (1986: Figs 10 and 5). The fact that one of the small dips occurs at the region of the precipitation is contrary to both the Frank *et al.* and the Sojka and Schunk patterns. The density configurations from these three passes suggest that the multicell patterns proposed by Frank *et al.*, which would have produced polar holes on the evening side of the noon–midnight meridian, were not correct for those conditions. In all three of the above passes this test does not, however, define the correct convection configuration.

CONCLUSIONS

This "blind" test of convection patterns using the ionospheric model demonstrates a preference for dis-

torted two-cell patterns in the majority of cases studied. Preference was determined by comparing the presence (or absence) and location of polar holes in measured data vs model predictions. While this test does not uniquely specify the best pattern, preference for distorted two-cell patterns rejects convection patterns which only circulate within the polar cap for B_y conditions and restricts shapes for B_y- conditions. As a corollary, convection patterns whose center circulates only within a dark polar cap must produce holes in the electron density. This means that electron density profiles can be used to exclude certain *ad hoc* convection models proposed to explain the data from a single pass; however, they cannot be used to derive unambiguously the correct model. Better statistics are needed for future evolution of patterns for B_z North, whether they be of the distorted two-cell or multicell variety.

REFERENCES

Banks, P. M., Araki, T., Clauer, C. R., St. Maurice, J. P. and Foster, J. C. (1984) The interplanetary electric field, cleft currents and plasma convection in the polar caps. *Planet. Space Sci.* **32**, 1551.

Burke, W. J., Kelley, M. C., Sagalyn, R. C., Smiddy, M. and Lai, S. T. (1979) Polar cap electric fields with northward interplanetary magnetic field. *Geophys. Res. Lett.* **6**, 21.

Clauer, C. R. and Banks, P. M. (1986) Relationship of the interplanetary electric field to the high latitude ionospheric field and currents: observations and model simulation. *J. geophys. Res.* **91**, 6959.

Clauer, C. R. and Friis-Christensen, E. (1988) High latitude dayside electric fields and currents during strong northward interplanetary magnetic field: observations and model simulation. *J. geophys. Res.* **93**, 2749.

Crooker, N. U. (1979) Dayside merging and cusp geometry. *J. geophys. Res.* **84**, 951.

Frank, L. A., Craven, J. D., Gurnett, D. A., Shawhan, S. D., Weimer, D. R., Burch, J. L., Winningham, J. D., Chappell, C. R., Waite, J. H., Heelis, R. A., Maynard, N. C., Sugiura, M., Peterson, W. K. and Shelley, E. G. (1986) The theta aurora. *J. geophys. Res.* **91**, 3177.

Hardy, D. A., Gussenhoven, M. S. and Holeman, E. (1985) A statistical model of auroral electron precipitation. *J. geophys. Res.* **90**, 4229.

Hedin, A. E., Reber, C. A., Newton, G. P., Spencer, N. W., Brinton, H. C., Mayr, H. G. and Potter, W. E. (1977) A global thermospheric model based on mass spectrometer and incoherent scatter data, MSIS-2. composition. *J. geophys. Res.* **82**, 2148.

Heelis, R. A., Reiff, P. H., Winningham, J. D. and Hanson, W. B. (1986) Ionospheric convection signatures observed by DE-2 during northward interplanetary magnetic field. *J. geophys. Res.* **91**, 5817.

Heppner, J. P. and Maynard, N. C. (1987) Empirical high

latitude electric field models. *J. geophys. Res.* **92**, 4467

Hoffman, R. A., Sugiura, M., Maynard, N. C., Candey, R. M., Craven, J. D. and Frank, L. A. (1988) Electrodynamic patterns in the polar region during periods of extreme magnetic quiescence. *J. geophys. Res.* **93**, 14,515.

Kan, J. R. and Burke, W. J. (1985) A theoretical model of polar cap auroral arcs. *J. geophys. Res.* **90**, 4171.

Killeen, T. L., Heelis, R. A., Hays, P. B., Spencer, N. W. and Hanson, W. B. (1985) Neutral motions in the polar thermosphere for northward interplanetary magnetic field. *Geophys. Res. Lett.* **12**, 159.

Krehbiel, J. P., Brace, L. H., Theis, R. F., Pinkus, W. H. and Kaplan, R. B. (1981) The *Dynamics Explorer* Langmuir Probe Instrument. *Space Sci. Instrum.* **5**, 493.

Maynard, N. C. (1974) Electric field measurements across the Harang discontinuity. *J. geophys. Res* **79**, 4620.

Maynard, N. C., Bielecki, E. A. and Burdick, H. F. (1981) Instrumentation for vector electric field measurements from *DE-B. Space Sci. Instrum.* **5**, 523.

Potemra, T. A., Zanetti, L. J., Bythrow, P. F., Lui, A. T. Y. and Iijima, T. (1984) B_z dependent convection patterns during northward interplanetary magnetic field. *J. geophys. Res.* **89**, 9753.

Reiff, P. H. and Burch, J L (1985) IMF by dependent plasma flow and Birkeland currents in the dayside magnetosphere: 2. A global model for northward and southward IMF. *J. geophys Res.* **90**, 1595.

Schunk, R. W. (1988) A mathematical model of the middle and high latitude ionosphere *Pageoph* **127**, 255

Schunk, R. W. and Raitt, W. J. (1980) Atomic nitrogen and oxygen ions in the daytime high-latitude F-region. *J geophys. Res.* **85**, 1255.

Schunk, R. W., Raitt, W. J. and Banks, P. M. (1975) Effect of electric fields on the daytime high-latitude E- and F-regions. *J. geophys. Res.* **80**, 3121.

Schunk, R. W. and Sojka, J. J. (1982) Ion temperature variations in the daytime high-latitude F-region. *J. geophys. Res.* **87**, 5169.

Schunk, R. W., Sojka, J. J. and Bowline, M. D. (1986) Theoretical study of the electron temperature in the high latitude ionosphere for solar maximum and winter conditions. *J. geophys. Res.* **91**, 12041.

Schunk, R. W. and Walker, J. C. G. (1973) Theoretical ion densities in the lower ionosphere. *Planet. Space Sci* **21**, 1875.

Sojka, J. J. (1989) Global scale, physical models of the F-region ionosphere: a review. *Rev Geophys.* **27**, 371

Sojka, J J., Raitt, W J. and Schunk, R W. (1981) A theoretical study of the high-latitude winter F-region at solar minimum for low magnetic activity *J geophys. Res* **86**, 609.

Sojka, J. J., Rasmussen, C. E. and Schunk, R. W. (1986) An IMF dependent model of the ionospheric convection electric field. *J. geophys. Res.* **91**, 11281.

Sojka, J. J. and Schunk, R W. (1987) Theoretical study of the high-latitude ionosphere's response to multicell convection patterns. *J. geophys. Res.* **92**, 8733

Spiro, R. W., Heelis, R. R. and Hanson, W. B. (1978) Ion convection and the formation of the mid-latitude F-region ionization trough. *J. geophys. Res* **83**, 4255.